Chemistry & Biology
Article

A Substrate-Inspired Probe Monitors Translocation, Activation, and Subcellular Targeting of Bacterial Type III Effector Protease AvrPphB

Haibin Lu,[1] Zheming Wang,[1,2] Mohammed Shabab,[3] Julian Oeljeklaus,[5] Steven H. Verhelst,[4,6] Farnusch Kaschani,[1,5] Markus Kaiser,[2,5] Matthew Bogyo,[4] and Renier A.L. van der Hoorn[1,2,*]
[1]Plant Chemetics Laboratory, Max Planck Institute for Plant Breeding Research, 50829 Cologne, Germany
[2]Chemical Genomics Centre of the Max Planck Society, 44227 Dortmund, Germany
[3]Max Planck Institute for Chemical Ecology, 07745 Jena, Germany
[4]Department of Pathology, Stanford School for Medicine, Stanford, CA 94305-5324, USA
[5]Center for Medical Biotechnology, Faculty of Biology, University of Duisburg-Essen, 45117 Essen, Germany
[6]Center for Integrated Protein Science Munich, Technical University of Munich, 85354 Freising, Germany
*Correspondence: hoorn@mpipz.mpg.de
http://dx.doi.org/10.1016/j.chembiol.2012.11.007

SUMMARY

The AvrPphB effector of *Pseudomonas syringae* is a papain-like protease that is injected into the host plant cell and cleaves specific kinases to disrupt immune signaling. Here, we used the unique substrate specificity of AvrPphB to generate a specific activity-based probe. This probe displays various AvrPphB isoforms in bacterial extracts, upon secretion and inside the host plant. We show that AvrPphB is secreted as a proprotease and that secretion requires the prodomain, but probably does not involve a pH-dependent unfolding mechanism. The prodomain removal is required for the ability of AvrPphB to trigger a hypersensitive cell death in resistant host plants, presumably since processing exposes a hidden acylation site required for subcellular targeting in the host cell. We detected two active isoforms of AvrPphB in planta, of which the major one localizes exclusively to membranes.

INTRODUCTION

Bacterial type III effectors are intriguing proteins. These prokaryotic proteins function in the eukaryotic host cell and have evolved to manipulate the cellular machinery of the host through intricate molecular mechanisms. Several of the type III effectors are papain-like cysteine proteases that belong to different families within the CA clan of the Merops protease database (Rawlings et al., 2012; Hotson and Mudgett, 2004). These proteins share a similar 3D structure, but the preferred substrate cleavage sites are remarkably different. For example, *Yersinia enterocolitica* YopT protease (family C58 of clan CA) cleaves host Rho-like GTPases (Shao et al., 2002), whereas Streptococcus pyogenes IdeS (family C66 of clan CA) specifically cleaves IgG antibodies (Wenig et al., 2004). Likewise, *Pseudomonas syringae* AvrRpt2 and AvrPphB (families C47 and C58 of clan CA, respectively) cleave the plant-specific RIN4 protein and host kinase PBS1, respectively (Mackey et al., 2003; Shao et al., 2003).

An interesting aspect of bacterial CA proteases is that these act in the host cytoplasm, whereas their host counterparts are encoded with signal peptides and act in lysosomes and in the endomembrane system (Turk et al., 2012). Consequently, bacterial CA proteases do not contain the disulphide bridges unlike their host counterparts, which are rigid proteases containing at least three disulphide bridges (Richau et al., 2012). Secretion through the narrow type III pilus also implies that bacterial CA proteases unfold during secretion and (re)fold in the host cytoplasm. Some bacterial CA proteases take advantage of eukaryotic posttranslational modifications for their activation and subcellular targeting. AvrRpt2, for example, is activated in the host by a host-derived cyclophilin (Coaker et al., 2005). Furthermore, fatty acid acylation of, e.g., AvrPphB and AvrRpt2, targets these proteases to the host membrane (Nimchuk et al., 2000; Dowen et al., 2009).

Folding, prodomain removal, and posttranslational modifications of bacterial CA proteases make it impossible to predict the subcellular and temporal activities of the different protease isoforms. Further studies on the function of these proteases therefore require new tools to detect activities of bacterial CA proteases. Activity-based protein profiling (ABPP) is a powerful technique to achieve this. ABPP of proteases is also called protease activity profiling and employs small molecule probes that react with the active site of proteases in a mechanism-dependent manner (Cravatt et al., 2008; Edgington et al., 2011; Serim et al., 2012). Labeling monitors the availability and reactivity of the active site, which correlates with protein activities (Kobe and Kemp, 1999). Various probes for different protease families have been introduced based on different reactive groups, including epoxide, vinyl-sulfone, and acyloxymethylketone (AOMK) (Edgington et al., 2011; Serim et al., 2012).

Proteases of the CA-clan select their substrates using residues residing at P2 and P3 positions (Turk et al., 2012). Most clan CA proteases prefer hydrophobic residues at the P2 positions, but there are exceptions. So far, selective probes for specific bacterial CA proteases based on selectivity for P2 and P3 residues have not been developed. Here, we exploited this strategy by developing a selective probe for the AvrPphB protease of *Pseudomonas syringae*, based on its selectivity for P2 and P3 residues.

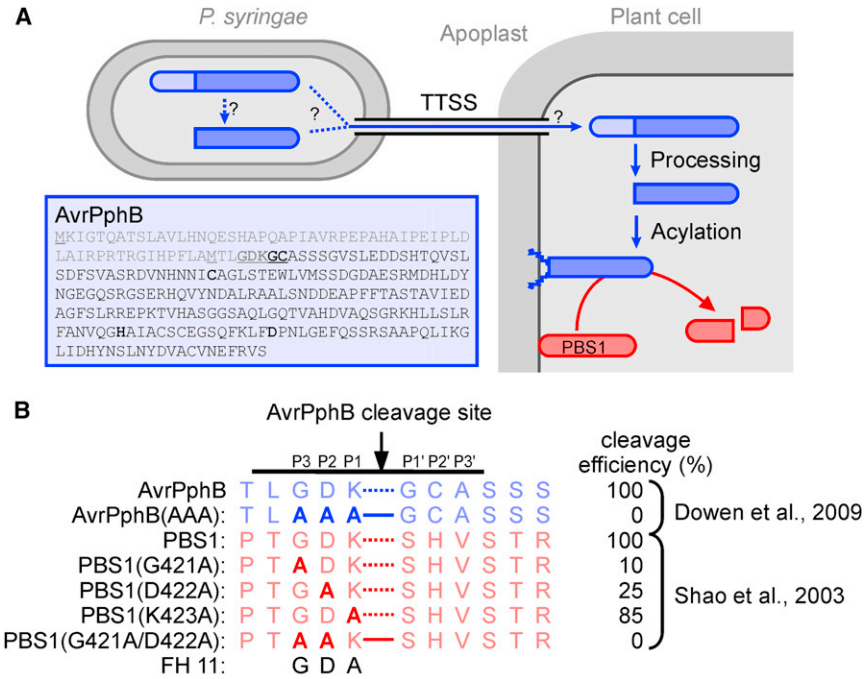

Figure 1. Design of a Specific Probe for AvrPphB

(A) Translocation, activation, and maturation of AvrPphB. Inset: protein sequence of AvrPphB, showing the prodomain (light gray) with two start codons (underlined) and the GDK cleavage site (bold underlined); and the mature protease domain (black), containing the acylation motif (bold underlined), and catalytic residues (bold). The cartoon shows the presumed events in AvrPphB processing, translocation, and acylation. TTSS, type III secretion system.

(B) Cleavage site specificity of AvrPphB. AvrPphB cleaves itself and PBS1 after the sequence GDK. Site-directed mutagenesis demonstrated that Gly at P3 and Asp at P2 are important recognition motifs for AvrPphB cleavage (Shao et al., 2003; Dowen et al., 2009).

(C) Structure of FH11 probe designed for AvrPphB. FH11 contains an AOMK-reactive group (red), a Gly-Asp-Ala peptide linker (blue) that provides specificity to target AvrPphB and a rhodamine reporter tag (yellow). The site of attack by the catalytic Cys of AvrPphB is indicated with a red arrowhead.

AvrPphB (Family C58 or clan CA) originates from the bean pathogen *Pseudomonas syringae* pv. *phaseolicola* (Jenner et al., 1991) and has been intensively studied by expression in *Pseudomonas syringae* pv. *tomato* DC3000 (PtoDC3000), which is pathogenic on the model plant *Arabidopsis thaliana* (Figure 1A; Katagiri et al., 2002; Quirino and Bent, 2003). AvrPphB is produced as a 35 kDa proprotease that autocatalytically converts to the 28 kDa mature isoform (Puri et al., 1997). AvrPphB is injected into the host through the type III secretion system (TTSS), and the N terminus of the mature protease becomes acylated with fatty acids in the host, which targets AvrPphB to the membrane, where the relevant substrates are located (Figure 1A; Nimchuk et al., 2000; Dowen et al., 2009). Although it is generally assumed that AvrPphB autocatalytically cleaves its own prodomain, it is not yet understood if this already occurs in bacteria or in the host cell. Further open questions are the role of the prodomain for correct folding of AvrPphB and how AvrPphB passes through the narrow type III pilus. Once located at the host membrane, AvrPphB cleaves host kinases PBS1, BIK1, and other *Arabidopsis* kinases (Shao et al., 2003; Zhang et al., 2010). Inactivation of some of these kinases suppresses immune signaling. Interestingly, some ecotypes of *Arabidopsis thaliana* carry immune receptor RPS5, which physically interacts with PBS1 to monitor AvrPphB-induced modification (Shao et al., 2003; Ade et al., 2007). PBS1 cleavage triggers RPS5 activation, resulting in hypersensitive cell death and effective immune responses (Shao et al., 2003; Ade et al., 2007; DeYoung et al., 2012). Alignment of the cleavage sites in AvrPphB and PBS1 revealed that AvrPphB cleaves after the tripeptide Gly-Asp-Lys (GDK, Figure 1B; Shao et al., 2003; Dowen et al., 2009). Site-directed mutagenesis of this tripeptide recognition site in PBS1 revealed that P3 = Gly and P2 = Asp are essential for cleavage specificity (Shao et al., 2003). The unique substrate binding specificity is explained by the charge and size of the substrate binding pockets for the P2 and P3 residues in the AvrPphB structure (Zhu et al., 2004).

Here, we took advantage of the unique substrate specificity of AvrPphB by designing probes carrying P3 = Gly and P2 = Asp. The probe was validated and used to study activities of AvrPphB isoforms in vitro, in *P. syringae* extracts, upon secretion and in planta. Using this approach, we could demonstrate that the prodomain is essential for AvrPphB secretion, but not for regulating AvrPphB activity. ProAvrPphB can be labeled but the removal of the prodomain is essential for hypersensitive response (HR)-inducing activity. Our studies uncover the regulation of activities of AvrPphB isoforms and give a proof of concept of successful probe design for specific clan CA proteases.

RESULTS

Specific Activity-Based Probe for AvrPphB

To develop a specific probe for AvrPphB, we produced a rhodamine-tagged Gly-Asp-Ala tripeptide followed by an

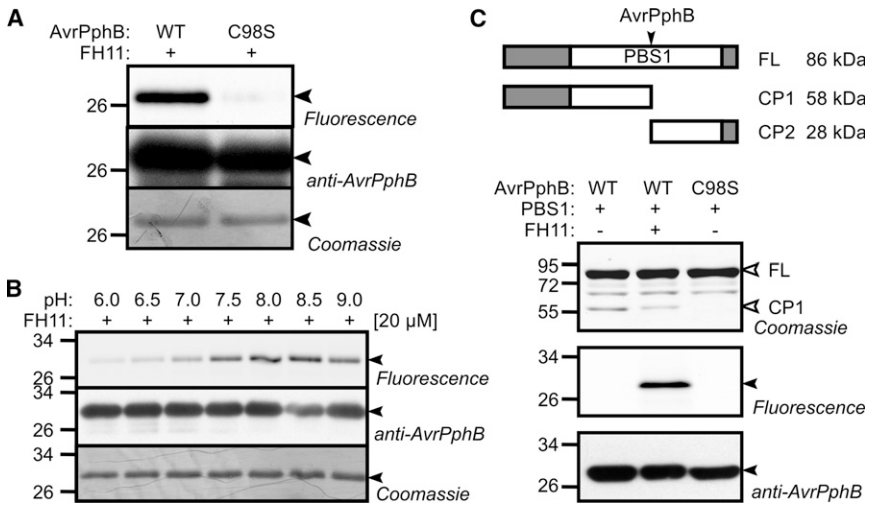

Figure 2. FH11 Labels and Inhibits AvrPphB at Cytoplasmic pH

(A) FH11 labels wild-type but not C98S AvrPphB. Wild-type and C98S mutant of His-tagged AvrPphB were produced in *E. coli* and purified. AvrPphB was incubated with 20 μM FH11 for 4 hr and detected by fluorescence scanning, western blot, and Coomassie staining.

(B) Labeling of AvrPphB is pH dependent. Purified AvrPphB was incubated with 20 μM FH11 at different pH for 2 hr and detected by fluorescence scanning, western blot, and Coomassie staining.

(C) FH11 inhibits AvrPphB-mediated cleavage of PBS1. Top: AvrPphB cleaves purified GST-PBS1(G252R)-His full-length (FL) into two cleavage products (CP): a 58 kDa CP1 and a 28 kDa CP2. Bottom: GST-PBS1(G252R)-His was incubated with AvrPphB in the presence or absence of 20 μM FH11 for 2 hr. Samples were analyzed by fluorescence scanning, western blot, and Coomassie staining.

AOMK-reactive group and named the probe FH11 (Figure 1C). FH11 labels mature AvrPphB produced and purified from *Escherichia coli*, and not the inactive AvrPphB mutant, which lacks the catalytic Cys residue (C98S; Shao et al., 2002) (Figure 2A). Labeling is optimal at neutral to slightly basic pH (Figure 2B), consistent with the activity of AvrPphB in the host cytoplasm. To test if FH11 also inhibits AvrPphB activity, we monitored cleavage of purified PBS1, produced in *E. coli* (Shao et al., 2003). Cleavage of PBS1 results in a 58 kDa cleavage product (CP1, Figure 2C). FH11 suppresses the accumulation of this product (Figure 2C), indicating that FH11 inhibits AvrPphB activity.

Activity Profiling of AvrPphB Produced by *P. syringae*

We next investigated if FH11 labels AvrPphB produced by *P. syringae*. For this, we produced plasmids expressing full-length AvrPphB with C-terminal His- and HA-epitope tags, respectively (Figure 3A). Infiltration of leaves of *Arabidopsis* carrying RPS5 with PtoDC3000 carrying the AvrPphB-encoding plasmids causes hypersensitive cell death within 20 hr upon infiltration (Figure 3A), indicating that both plasmids encode active AvrPphB.

Labeling of extracts of *P. syringae* containing the AvrPphB-encoding plasmids causes a strong, specific signal at 28 kDa, representing mature AvrPphB, and a weaker 34 kDa signal, representing ProAvrPphB (Figure 3B). No signals were detected in the empty vector (EV) control (Figure 3B), indicating that this probe is highly specific for AvrPphB. Both His- and HA-tagged AvrPphB are labeled, and AvrPphB-HA migrates at slightly higher molecular weight, probably because of the slightly larger epitope tag (Figure 3B). Labeling is absent if no reducing agent is added (Figure 3C), and labeling is suppressed by preincubation with E-64 and with GDA-AOMK, a nonfluorescent version of FH11 (Figure 3D). A time course of labeling showed that 4 hr is needed to reach maximum labeling (Figure 3E). Labeling at different probe concentrations indicates that labeling is saturated with 20 μM FH11 (Figure 3F). Labeling is optimal at neutral pH, but, in contrast to purified recombinant AvrPphB expressed in *E. coli* (Figure 2B), the AvrPphB-HA protein is only stable at neutral pH (Figure 3G). For all subsequent experiments, labeling was performed with 20 μM FH11 for 4 hr at pH 7.0, unless otherwise indicated. Taken together, these data demonstrate that FH11 is a highly specific activity-based probe for AvrPphB in extracts of *P. syringae*.

Type III Secretion of AvrPphB

We next tested if FH11 detects AvrPphB secreted through the TTSS. Bacteria were grown in minimal medium (MM) to induce the TTSS and centrifuged to separate the secreted proteins (supernatant) from the bacteria (pellet). FH11 labeling revealed AvrPphB-HA activity in extracts of the bacterial pellet and in the supernatant (Figure 4A), indicating that AvrPphB-HA is secreted. Surprisingly, poor labeling of AvrPphB-His was detected in the supernatant, though it was clearly detected in the bacterial pellet (Figure 4A). These data indicate that AvrPphB-His is poorly secreted, in contrast to AvrPphB-HA.

To determine if AvrPphB secretion is TTSS dependent and not caused by cell lysis, we expressed AvrPphB-HA in the *ΔhrcC* mutant of PtoDC3000, which lacks a functional TTSS (Penaloza-Vazquez et al., 2000). In contrast to wild-type bacteria, AvrPphB-HA labeling is no longer detected in the medium of the *ΔhrcC* mutant (Figure 4B), confirming that we detected activity of AvrPphB secreted through the TTSS.

Stability of AvrPphB Structure at Various pH

We detected an efficient secretion of AvrPphB through the TTSS. This is remarkable since AvrPphB is a globular protein with a diameter of >3.5 nm, which is too large to pass through the narrow type III pilus. Since pH has a drastic effect on AvrPphB activity and stability (Figures 2B and 3G), we investigated if the structure is dependent on pH, similar to what was found previously for AvrPto, which unfolds at apoplastic pH (Dawson et al., 2009). The crystal structure of AvrPphB at pH 6.7 (Zhu et al., 2004) shows that AvrPphB consists of 39% α helix and 28% β sheet (Figure 5A). CD spectroscopy at pH 5, 6, and 7 showed spectra that are consistent with this secondary structure, whereas some of the α helixes seem to unfold at pH 8 and 9 (Figure 5B). These data indicate that at apoplastic and neutral pH (pH 5–7), AvrPphB does not undergo significant

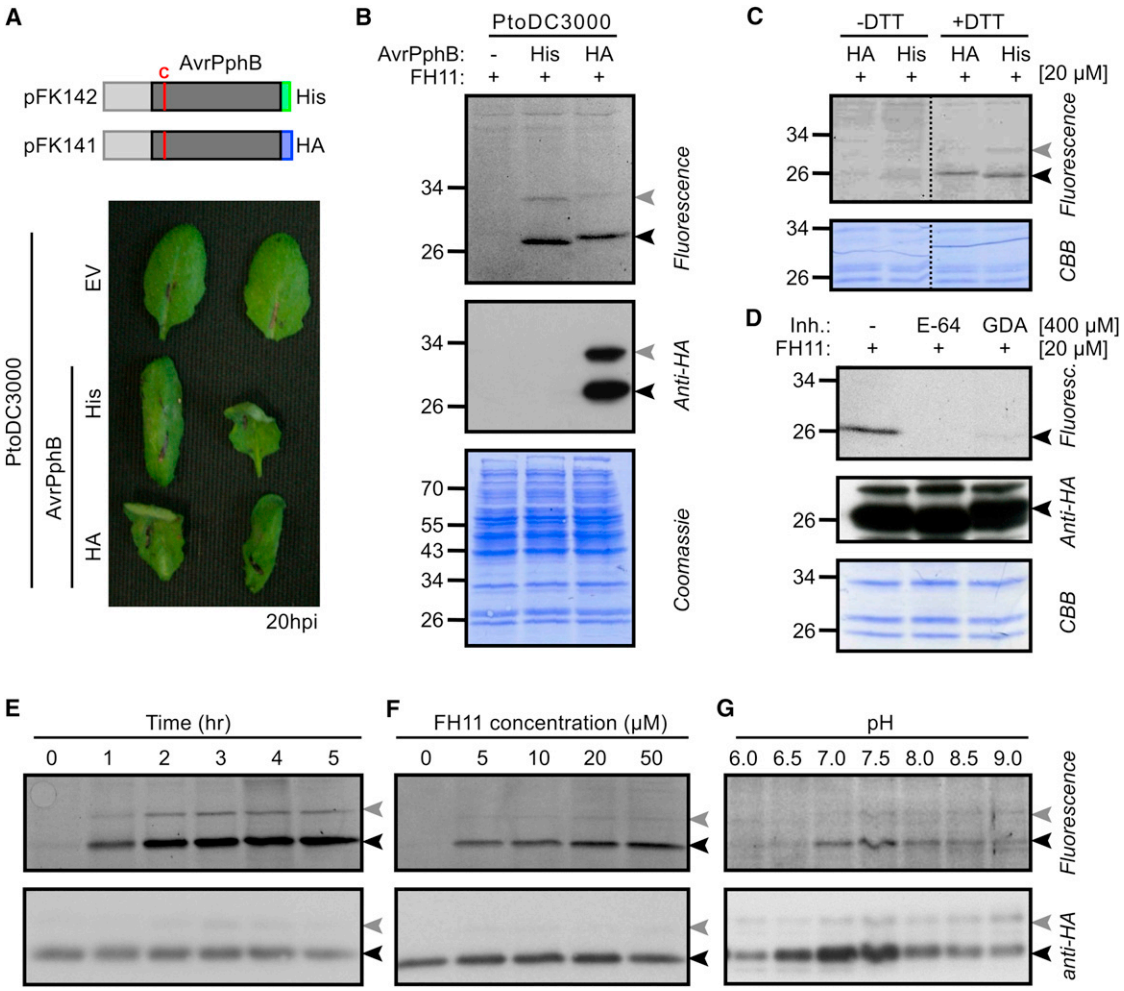

Figure 3. FH11 Labels AvrPphB Expressed by *P. syringae*

(A) C-terminally tagged AvrPphB is active when expressed in *P. syringae*. Top: plasmids pFK141 and pFK142 encode C-terminally HA- and His-tagged full length AvrPphB, respectively. Light gray, AvrPphB prodomain; dark gray, mature AvrPphB protease domain with catalytic cysteine (C). Bottom: *P. syringae* pv. *tomato* DC3000 (PtoDC3000) carrying the empty vector (EV) or AvrPphB-encoding plasmids were infiltrated into wild-type *Arabidopsis* ecotype Col-0 at 10^8 bacteria/ml and pictures were taken 20 hr later, showing tissue collapse caused by both AvrPphB-producing strains.

(B) FH11 labels AvrPphB expressed in *P. syringae*. Extracts of PtoDC3000 producing AvrPphB-His or AvrPphB-HA were incubated with 20 μM FH11 for 4 hr and analyzed by in-gel fluorescence scanning and western blot.

(C) DTT dependency of labeling. Extracts of PtoDC3000 producing HA- and His-tagged AvrPphB were incubated with 20 μM FH11 in the absence or presence of 1 mM DTT for 4 hr. Samples were analyzed by in-gel fluorescence scanning. CBB, Coomassie brilliant blue.

(D) FH11 labeling of AvrPphB is blocked with E-64 and GDA-AOMK. Extracts of PtoDC3000 producing AvrPphB-HA were preincubated with 400 μM E-64 or GDA-AOMK for 1 hr and then labeled with 20 μM FH11 for 4 hr. Samples were analyzed by in-gel fluorescence scanning and western blot. CBB, Coomassie brilliant blue; inh, inhibitor.

(E) Time course of FH11 labeling. Extracts of PtoDC3000 producing AvrPphB-HA were incubated with 20 μM FH11 for various time points. Samples were analyzed by in-gel fluorescence scanning and western blot.

(F) Labeling of AvrPphB at various probe concentrations. Extracts of PtoDC3000 producing AvrPphB-HA were incubated with various FH11 concentrations for 4 hr. Samples were analyzed by in-gel fluorescence scanning and western blot.

(G) Labeling of AvrPphB at various pH. Extracts of PtoDC3000 producing AvrPphB-HA were incubated with FH11 at various pH for 4 hr. Samples were analyzed by in-gel fluorescence scanning and western blot.

changes in its secondary structure, implying that other unfolding mechanisms are involved in AvrPphB secretion.

The Prodomain Is Essential for Secretion, but Not for Folding

To determine the role of the prodomain and prodomain removal in secretion and HR-inducing activity, we generated an AvrPphB mutant lacking the prodomain AvrPphB(Δ62) (Figure 6A). Labeling and protein blot analysis revealed that the AvrPphB(Δ62) protein accumulates as a 28 kDa mature protein and can be labeled with FH11 (Figure 6B). However, the protein can no longer be detected in the medium (Figure 6B), indicating that the prodomain is required for secretion. PtoDC3000 producing the AvrPphB(Δ62) mutant is unable to trigger HR

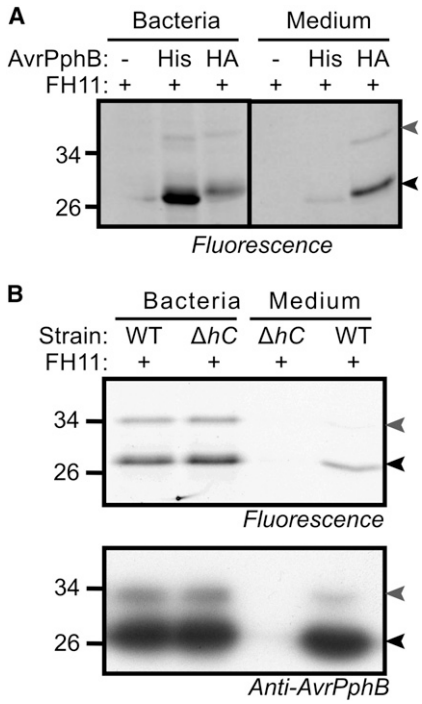

Figure 4. Type III Secretion of AvrPphB

(A) FH11 labeling of bacterial extracts and medium. Bacteria containing empty vector (–) or plasmids encoding AvrPphB-His or AvrPphB-HA were grown in minimal medium and centrifuged to separate bacteria (pellet) from medium (supernatant). Bacterial extracts and medium were labeled with FH11 and labeled proteins detected by in-gel fluorescence.

(B) Active AvrPphB in medium is dependent on type III secretion system. AvrPphB-HA was produced in wild-type (WT) and *ΔhrcC* (*ΔhC*) mutant PtoDC3000 bacteria when grown in minimal medium. The supernatant and bacterial pellet were labeled with FH11 and analyzed by in-gel fluorescence and western blotting.

when infiltrated in *Arabidopsis* leaves (Figure 6C), consistent with the inability to secrete AvrPphB.

Prodomain Removal Is Required for HR-Inducing Activity

To determine the importance of prodomain removal for secretion and triggering HR, we generated the AvrPphB(AAA) mutant, which carries three alanines instead of the GDK cleavage site (Figure 6A). In contrast to wild-type AvrPphB(GDK) protein, the AvrPphB(AAA) protein accumulates at 34 kDa, indicating that the prodomain can no longer be removed (Figure 6D). Labeling of this protein with FH11 indicates that this protein is nevertheless active (Figure 6D). Importantly, the proprotease of AvrPphB(AAA) is efficiently secreted into the medium of wild-type bacteria but not of *ΔhrcC* bacteria (Figure 6D), demonstrating that ProAvrPphB is secreted through the TTSS. A weak signal at 28 kDa in the bacterial pellet is presumably caused by translation from the second start codon, rather than by cleaved AvrPphB(AAA) (Dowen et al., 2009). The weak 25 kDa signals in the medium of AvrPphB(AAA)-expressing bacteria migrate with a lower molecular weight than mature AvrPphB(GDK) (Figure 6D) and are presumably caused by improper prodomain removal. Importantly, PtoDC3000 producing the AvrPphB(AAA) mutant is unable to trigger HR when infiltrated in *Arabidopsis* leaves (Figure 6C), indicating that the removal of the prodomain is essential to trigger HR.

Two Isoforms of AvrPphB Reside at Different Locations *In Planta*

We next investigated if FH11 labeling detects AvrPphB activity in host cells. For this, we transiently expressed AvrPphB-HA in *Nicotiana benthamiana* by infiltration of *Agrobacterium tumefaciens* carrying plasmids containing DEX-inducible AvrPphB (Shao et al., 2003). FH11 labeling of extracts from agroinfiltrated leaves revealed a doublet signal at 28 kDa in samples expressing AvrPphB, in addition to several host-derived signals at 34–36 kDa (Figure 7). Subcellular fractionation shows that the lower isoform locates in the membrane fraction, whereas the upper isoform locates in both the soluble and membrane fractions (Figure 7). Thus, FH11 labeling displays the subcellular location of two AvrPphB isoforms present in planta.

DISCUSSION

AvrPphB is an intriguing bacterial Cys protease that acts in the cytoplasm of the eukaryotic host cell where it cleaves PBS1 and other host kinases. Using the unique substrate specificity of AvrPphB, we have designed, synthesized, and validated an activity-based probe and displayed the activities of the different AvrPphB isoforms in *P. syringae*, upon secretion and in the plant cell. We detected two active AvrPphB isoforms in planta and revealed that the prodomain is required for secretion and that its removal is required for inducing HR.

Activity-Based Profiling of AvrPphB with Selective AOMK Probe

Labeling experiments illustrate that FH11 labeling reflects the activity of the AvrPphB isoforms, rather than their presence. For example, labeling of AvrPphB by FH11 requires a reducing agent, the absence of AvrPphB inhibitors, and neutral pH. Furthermore, FH11 does not label the inactive C98S mutant AvrPphB protein and FH11 inhibits AvrPphB in PBS1 cleavage assays. The optimal labeling conditions coincide with the conditions of the host cytoplasm.

The specificity of FH11 is illustrated by the fact that AvrPphB activity can be detected in plant extracts, despite the presence of many other plant cysteine proteases. Probes carrying AOMK-reactive groups have previously been used to target CD-clan cysteine proteases (legumains, caspases, and gingipains) that carry specific residues at the P1 position (Kato et al., 2005). However, AOMK probes that target bacterial CA-clan proteases by using specific residues at P2 and P3 positions have not been reported earlier. This study demonstrates that substrate-based probe design can be a successful strategy for bacterial CA proteases. Interestingly, the bacterial type III CA proteases ORF4, NopT, and RipT cleave after the motifs VER, DKM, and PLR, respectively, suggesting that different substrate-inspired probes can be generated to study these proteins (Dowen et al., 2009).

A unique advantage of protease activity profiling is that this technique displays activities of different isoforms. We found that, besides mature AvrPphB, ProAvrPphB is also efficiently

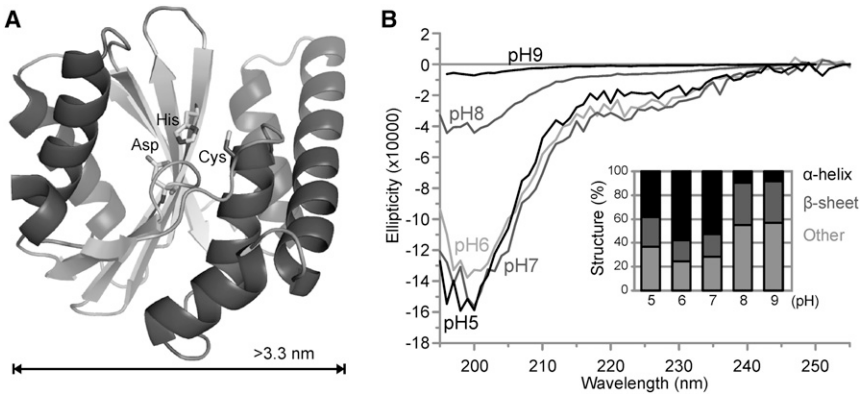

Figure 5. AvrPphB Has a Papain-like Structure at Acidic and Neutral pH

(A) Crystal structure of AvrPphB (Protein Data Bank code: 1UKF) showing the Cys-His-Asp catalytic triad (sticks) flanked between the β sheet lobe (left) and the α helix lobe (right). The structure contains seven antiparallel β sheets (28% of the mature protein) and six α helixes (39% of the mature protein).

(B) CD spectroscopy of mature AvrPphB at different pH. CD spectra were recorded for purified AvrPphB at various pH. Secondary structures were calculated by CDPro and K2d.

labeled with FH11. This implies that the active site cysteine is available and reactive toward FH11. These data indicate that also ProAvrPphB is an active protease. Alternatively, the prodomain blocks the entry for protein substrates, but not for small molecules.

Prodomain Is Required for Secretion but Not for Folding or Stabilization of AvrPphB

We found that deletion of the prodomain abolishes HR-inducing activity on *Arabidopsis* carrying RPS5. These data are consistent with the observation that deletion of the prodomain of AvrPphB abolished the avirulence function of AvrPphB in pv *phaseolicola* 1448A on bean plants carrying the corresponding *R3* resistance gene (Tampakaki et al., 2002). Importantly, we have demonstrated that AvrPphB(Δ62) accumulates as a mature protein that can be labeled by FH11, excluding the possibility that the prodomain is required for stabilization or proper folding of AvrPphB. However, the deletion mutant is no longer secreted into the medium. This indicates that the prodomain is required for AvrPphB secretion and explains why these mutants have lost HR-inducing activity.

We also demonstrated that ProAvrPphB is effectively secreted by the TTSS. This was especially evident from the studies using the AvrPphB(AAA) cleavage mutant, which is effectively secreted in a TTSS-dependent manner. These data are consistent with the fact that the prodomain contains a type III secretion signal (EffectiveT3 Score = 0.99979; Arnold et al., 2009). Thus, although the prodomain is not required to create active AvrPphB in bacteria, it is essential for secretion by the TTSS.

Prodomain Removal Is Essential for HR-Inducing Activity

We found that the AvrPphB(AAA) cleavage mutant is unable to trigger HR in RPS5-containing plants, despite the high levels of secreted ProAvrPphB that can be labeled by FH11. There can be several explanations for this phenomenon. First, although ProAvrPphB can be labeled with FH11, it may not be able to cleave PBS1 because of steric interference by the prodomain. Alternatively, the presence of the prodomain blocks the acylation of AvrPphB, resulting in mislocalization. The essential role of acylation was also demonstrated by the fact that mutants in the acylation motif are unable to trigger HR (Dowen et al., 2009). These observations indicate that, besides secretion, the removal of the prodomain is also required to create a proper acylation site that is required for subcellular targeting.

Folding and pH Sensitivity of AvrPphB

ProAvrPphB is effectively secreted through the TTSS. This is remarkable since the type III pilus is probably too narrow (<2.5 nm; Loquet et al., 2012) to allow translocation of folded AvrPphB (>3.5 nm; Zhu et al., 2004). Type III effector proteins are generally thought to pass the pilus as partly unfolded proteins and fold in the host cytoplasm. Chaperones are frequently mediating the unfolding of type III effectors (Johnson et al., 2005). YopT, for example, the AvrPphB homolog from Yersinia, is accompanied by chaperone SycT (Iriarte and Cornelis, 1998). However, no chaperone has been described for AvrPphB. The closest SycT homolog in *P. syringae* pv. *phaseolicola* 1448A is ShcF, but this is the chaperone of AvrPphF (Singer et al., 2004). Although the type III effector AvrPto can unfold itself, depending on pH (Dawson et al., 2009), we did not detect pH-dependent unfolding of AvrPphB at apoplastic pH. The unfolding and folding of AvrPphB during translocation remains an interesting subject for future studies.

Acylation of AvrPphB *In Planta*

FH11 labeling displayed the two isoforms of AvrPphB in planta. The lower MW isoform is located in membranes and is therefore presumably acylated. The higher MW isoform occurs both in the soluble and membrane fractions and may represent a nonacylated isoform. The higher MW suggests that this isoform is not mature, which would be consistent with the absence of acylation. Mutagenesis of the acylation motif, combined with FH11 labeling and subcellular fractionation studies, is required to elucidate the identity of the different AvrPphB isoforms. The targeting of this bacterial CA protease to the host membrane is distinct from the host CA-clan proteases of the host since these are all soluble proteins.

SIGNIFICANCE

The work presented here demonstrates that specific probes for bacterial CA proteases can be inspired on their unique P2 and P3 cleavages site specificities. This principle was shown here for the AvrPphB protease of the plant pathogenic *Pseudomonas syringae* by combining a tripeptide containing residues present in AvrPphB substrates with an

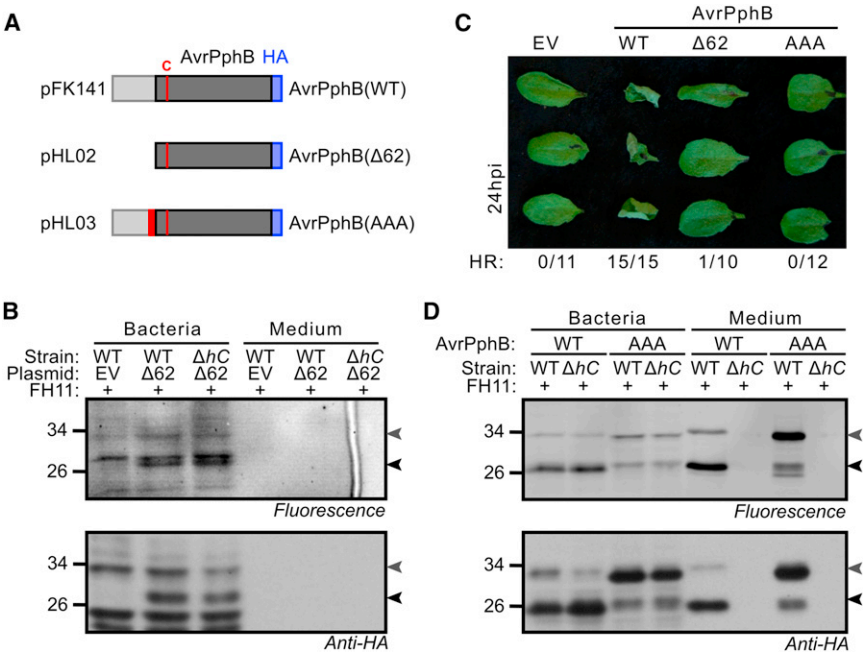

Figure 6. Secretion and HR Induction Require a Removable Prodomain

(A) AvrPphB mutants generated for these studies. Wild-type AvrPphB contains the GDK cleavage motif at the end of the prodomain. The prodomain is deleted in the AvrPphB(Δ62) mutant and the GDK motif is mutated into AAA in the AvrPphB(AAA) mutant.

(B) Prodomain removal blocks AvrPphB secretion. Wild-type and *ΔhrcC* (*ΔhC*) mutant PtoDC3000 bacteria carrying empty vector (EV) or the AvrPphB(Δ62) mutant were grown in minimal medium. Proteins were extracted from the cell pellet and medium, labeled with FH11 and analyzed by in-gel fluorescence scanning and western blotting.

(C) Deletion of the prodomain and removal of the GDK cleavage motif prohibit HR-inducing activity. *P. syringae* pv. *tomato* DC3000 (PtoDC3000) carrying the empty vector (EV) or AvrPphB-encoding plasmids were infiltrated into wild-type *Arabidopsis* ecotype Col-0 at 10^8 bacteria/ml and pictures were taken 24 hr later, showing tissue collapse. Frequency of HR observed in infiltrated leaves is indicated at the bottom.

(D) Processing site mutant accumulates in the proform but is still secreted. Wild-type and *ΔhrcC* (*ΔhC*) mutant PtoDC3000 bacteria expressing wild-type (GDK) or mutant (AAA) AvrPphB-HA were grown in minimal medium. Proteins were extracted from the cell pellet and medium, labeled with FH11 and analyzed by in-gel fluorescence scanning and western blotting.

acyloxymethylketone-reactive group and a bodipy fluorescent reporter group. We used this probe to study the activity of AvrPphB in bacteria, upon secretion and inside host cells. This work revealed that AvrPphB is secreted as a proprotease that can be labeled with our probe. The secretion through the narrow type III pilus implies that AvrPphB unfolds, but pH-dependent unfolding was not detected for AvrPphB, implying that other mechanisms facilitate AvrPphB secretion. The prodomain is required for secretion and its removal is essential for the induction of the hypersensitive cell death response in plants carrying the RPS5 immune receptor. Taken together, this work illustrates that specific activity-based probes for bacterial CA proteases can be generated and used to study aspects of their activation and function during pathogenesis.

EXPERIMENTAL PROCEDURES

Synthesis of FH11 and GDA-AOMK

The synthesis of FH11 was performed as described (Kato et al., 2005). In brief, *N*-methyl morpholine (686 μl, 6.25 mmol) and *iso*-butylchloroformiate (752 μl, 5.75 mmol) were added to a 0.2 M solution of Fmoc-Ala-OH (1.65 g, 5 mmol) in anhydrous THF at −10°C, and the resulting mixture was stirred for 25 min. Etheral diazomethane (20 mmol) was generated in situ, using the procedure described in the Aldrich Technical Bulletin AL-180, and added to the stirred solution of the above prepared mixed anhydride at 0°C and stirred for 3 hr. To obtain the chloromethyl ketone, a solution of conc. HCl in acetic acid (1:1, 15 ml) was then added dropwise to the reaction mixture at 0°C. Ethyl acetate was added and the organic layer was separated, washed with water and brine, and dried over Na_2SO_4. Evaporation of the solvent yielded a white product (1.82 g) that was used without further purification for loading on a hydrazide resin. To this end, a 0.5 M solution of Fmoc-Ala-CMK (1 g, 2.9 mmol) in dimethylformamide (DMF) was added to the hydrazide resin (2.2 g, 1.1 mmol/g initial loading) and shaken for 3 hr at 50°C. The reaction mixture was removed, the resin was washed with DMF, and a 0.5 M solution of 2,6-dimethyl benzoic acid (750 mg, 5 mmol) and KF (580 mg, 10 mmol) in DMF were added to the resin. The resin was shaken at room temperature overnight, the reaction mixture was removed again, and the resin was washed extensively. The loading of the resin was determined via the Fmoc-cleavage method (resulting in a loading of 0.565 mmol/g) and was used as the basis for the calculation of reagent equivalents in the later coupling steps. For the subsequent coupling of the amino acids and the rhodamine fluorophore, standard Fmoc SPPS conditions were used, i.e., the loaded resin (100 mg, 0.057 mmol); 3 eq. of Fmoc-Asp(O*t*Bu)-OH, Fmoc-Gly-OH, or Fmoc-Ahx-OH; 3 eq. of HOBt; 3 eq. of DIC and 1 eq. of triethylamine; for Fmoc cleavage, 20% piperidine in DMF was used; for coupling of the rhodamine residue, 1.5 eq of Rh-OSu was employed. The product was cleaved from the resin with 95% TFA/2.5% water/2.5% TIS and purified by RP-HPLC, thereby yielding 6.2 mg (6 μmol, 11%) of a violet solid. Electrospray ionization-liquid chromatography-mass spectrometry analysis confirmed the identity of the synthesized compound: t_R = 8.01 min, *m/z* = 1038.16 calcd. for $C_{58}H_{65}N_6O_{12}$ $[M+H]^+$, found: 1,037.80.

Plant Materials

Arabidopsis thaliana ecotype Col-0 was grown at 22°C at 10 hr light/day and 60% relative humidity and used when 5 weeks old for HR assays at 20°C. *Nicotiana benthamiana* was grown at 20°C at 14 hr light/day at 80% relative humidity and used before flowering.

Construction of Plasmids

AvrPphB was amplified from the PtoDC3000 strain carrying AvrPphB (Simonich and Innes, 1995) by PCR using gene-specific primers 5′-atcgggatccaggaggacagctatgaaaataggtacgcaggccacctcgc-3′ (carries ribosome binding site) and 5′-gcatctcgagttacgcataatccggcacatcatcaggatacgaaactctaaactcgttacgc-3′ (HA-tag) or 5′-gcatctcgagttactgatggtgatggtgatgcgaaactctaaactcgttacgc-3′ (His-tag) and cloned into pBlueScript using BamHI and XhoI restriction enzymes, resulting in pFK131 and pFK132, respectively. The inserts were verified by sequencing and shuttled into pML123 (Labes et al., 1990) using BamHI and XhoI restriction sites, resulting in pFK141 (AvrPphB-HA) and pFK142 (AvrPphB-His), respectively. AvrPphB(Δ62) and AvrPphB(AAA) mutants were made by site-direct mutagenesis using pFK131 as template. 5′-ggatccaggaggacagctatggggtgtgcatcctcttcag-3′ and 5′-ctgaagaggatgcacaccccatagctgtcctcctggatcc-3′ were used to make AvrPphB(ΔN62), while

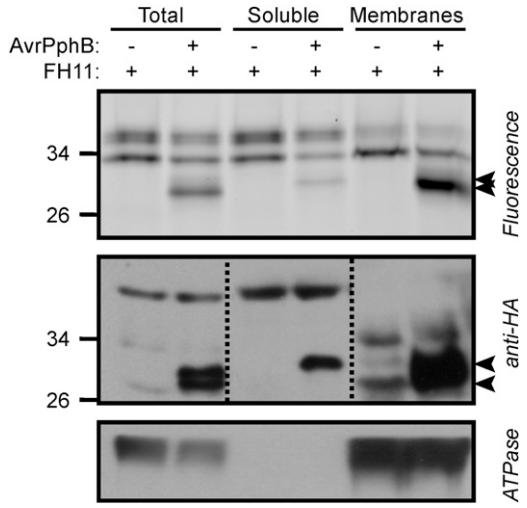

Figure 7. FH11 Detects Two Active Isoforms of AvrPphB In Planta
FH11 labels AvrPphB produced by agroinfiltration. *N. benthamiana* leaves were agroinfiltrated with or without Dex-inducible AvrPphB. After 48 hr, leaves were sprayed with 50 μM Dex. Proteins were extracted at 6 hr after Dex treatment. Total fraction was separated into a soluble fraction and a membrane fraction by ultracentrifugation, and the three fractions were labeled with FH11 and analyzed by in-gel fluorescence scanning and western blot.

5′-cattcctggcaatgacactggcagcagcagggtgtgcatcctcttc-3′ and 5′-gaagaggatgc acaccctgctgctgccagtgtcattgccaggaatg-3′ were used to make AvrPphB(AAA). Then, AvrPphB fragments were cloned into pML123 using BamHI and XhoI restriction sites resulting in pHL02 and pHL03, respectively. Plasmids were transformed into PtoDC3000 and PtoDC3000(*ΔhrcC*) by electroporation. GST-PBS1(G252R)-His (pHL01) was made by site-directed mutagenesis using GST-PBS1-His (Shao et al., 2003) as template and using primers 5′-ctcatgtctccactagagttatgcgaacttatggttattgtgctcc-3′ and 5′-ggagcacaataacca taagttcgcataactctagtggagacatgag-3′. The sequence was verified and the plasmid transformed into *E. coli* BL21 for protein expression.

Protein Expression and Purification
Recombinant AvrPphB-His, AvrPphB(C98S)-His, and GST-PBS1(G252R)-His were expressed in *E. coli* BL21 cells. Bacteria were grown in lysogeny broth medium containing 50 μg/μl ampicillin until OD_{600} = 0.6–1. Protein expression was induced overnight in the presence of 0.5 mM IPTG at 20°C. Cells were sonicated (5 min) in lysis buffer (20 mM Tris [pH 8.0], 200 mM NaCl, 20 mM imidazole, 5% glycerol, 10 mM β-mercaptoethanol, and 1 mM PMSF). All proteins were purified on Ni-NTA agarose (QIAGEN) and eluted with the same buffer without PMSF containing 250 mM imidazole, as described previously (Shao et al., 2003). Protein concentrations were determined using Bradford Protein Assay (BioRad).

PBS1 Cleavage Assay
Recombinant, purified AvrPphB-His (100 ng) was preincubated with 20 μM FH11 in 50 mM Tris (pH 7.5), 5 mM DTT at room temperature for 3 hr. Purified GST-PBS1(G252R)-His (6 μg/reaction) was added and incubation continued at 30°C for 2 hr. Samples were analyzed by Coomassie staining, western blot, and fluorescence scanning.

Transient Expression in *Nicotiana benthamiana* and Membrane Isolation
Overnight-grown *Agrobacterium tumefaciens* cultures (strain GV3101) carrying plasmids with dexamethasone-inducible AvrPphB were resuspended in infiltration buffer (10 mM MES [pH 5], 10 mM $MgCl_2$, and 1 mM acetosyringone). The optical density at 600 nm was adjusted to 2, and cultures carrying AvrPphB-expressing vectors were mixed with cultures carrying p19-expressing vectors. Cultures were incubated for 3 hr at room temperature. These cultures were infiltrated into fully expanded leaves of 4- to 6-week-old *N. benthamiana* plants. Infiltrated leaves were sprayed with 50 μM dexamethasone at 48 hr postinfiltration. Samples were collected for protein extractions 6 hr after dexamethasone application. For membrane isolation, 3 g fresh leaves were ground in buffer (25 mM Tris [pH 7.5], 3% PVPP, 250 mM sucrose). After filtering through two layers of miracloth, the filtrate was centrifuged at 4°C 4,000 rpm for 20 min. Membranes were collected from the supernatant by centrifugation at 100,000 × *g* for 1 hr. The pellet (membrane fraction) was resuspended in 25 mM Tris (pH 7.5) and 250 mM sucrose, and a sample from the supernatant was taken as soluble fraction (SF). The total, soluble, and membrane fractions were further analyzed with FH11 labeling. The anti-ATPase antibody was purchased from Agrisera.

Effector-Secretion Assay
Wild-type and *ΔhrcC* strains of PtoDC3000 carrying AvrPphB were grown in NYG medium containing 5 μg/μl gentamicin at 28°C for overnight. Bacteria were collected and resuspended in 20 ml MM containing 10 mM fructose (Huynh et al., 1989) to OD_{600} = 0.2 and grown for 20 hr at 20°C. Cells were harvested by centrifugation at 2,000 × *g* for 10 min, while supernatants were concentrated using 3,000 MWCO filters (Millipore). The bacterial pellet was resuspended in the same volume as the concentrated supernatant and both samples were used for FH11 labeling.

HR Assay
PtoDC3000 bacteria were grown overnight in NYG medium containing 5 μg/μl gentamicin at 28°C. Bacteria were collected, washed, and resuspended in water at OD_{600} = 0.1. The bacterial suspensions were infiltrated into leaves of *Arabidopsis thaliana* ecotype Col-0. Pictures were taken 20 hr after inoculation.

FH11 Labeling
For FH11 labeling of AvrPphB produced in PtoDC3000 extracts, 50 μg protein was incubated with 20 μM FH11 in 40 μl total volume containing 50 mM Tris (pH 7.5) and 2 mM DTT at room temperature in the dark for 4 hr. The samples were separated on 12% SDS-PAGE gel and analyzed by Typhoon 9000 scanner (GE Healthcare) and/or western blot with anti-HA or anti-AvrPphB antibody (Dowen et al., 2009). For labeling AvrPphB expressed in leaves, 100 μg total leaf extracts, soluble fractions, and membrane fractions were incubated with 20 μM FH11, 50 mM Tris (pH 7.5), 2 mM DTT in 40 μl total volume at room temperature in the dark for 4 hr. The samples were analyzed the same as labeling AvrPphB produced in PtoDC3000. For labeling AvrPphB purified from BL21, the method is the same as FH11-labeling leaf extracts except 1 μg purified AvrPphB was used.

Circular Dichroism Measurement
The circular dichroism (CD) spectra were recorded on a J-715 spectropolarimeter with a PTC343 Peltier unit (Jasco, Tokyo) at room temperature in a quartz cuvette. All spectra were corrected for buffer contributions and observed values were converted to molar ellipticity. Each CD spectrum was accumulated from eight scans at 50 nm/min with a 1 nm slit width and a time constant of 1 s for a nominal resolution of 1 nm. Microcolumns (Vivaspin 500) were used to exchange different buffers for pH of the AvrPphB. Secondary structures were calculated by CDPro and K2d programs.

ACKNOWLEDGMENTS

We would like to thank Dr. Jack Dixon for sending the AvrPphB antibody and the *E. coli* and *A. tumefaciens* strains for producing (mutant) AvrPphB and PBS1, Dr. Jim Alfano for providing pML123, and Dr. Roger Innes for sharing strains for transient expression of DEX-inducible (mutant) AvrPphB. This work was financially supported by the Max Planck Society and by the Deutsche Forschungsgemeinschaft (DFG project HO 3983/3-3). M.K. greatly acknowledges support from an ERC Starting Grant (grant No. 258413).

Received: October 17, 2012
Revised: November 21, 2012
Accepted: November 22, 2012
Published: February 21, 2013

REFERENCES

Ade, J., DeYoung, B.J., Golstein, C., and Innes, R.W. (2007). Indirect activation of a plant nucleotide binding site-leucine-rich repeat protein by a bacterial protease. Proc. Natl. Acad. Sci. USA *104*, 2531–2536.

Arnold, R., Brandmaier, S., Kleine, F., Tischler, P., Heinz, E., Behrens, S., Niinikoski, A., Mewes, H.W., Horn, M., and Rattei, T. (2009). Sequence-based prediction of type III secreted proteins. PLoS Pathog. *5*, e1000376.

Coaker, G., Falick, A., and Staskawicz, B. (2005). Activation of a phytopathogenic bacterial effector protein by a eukaryotic cyclophilin. Science *308*, 506–508.

Cravatt, B.F., Wright, A.T., and Kozarich, J.W. (2008). Activity-based protein profiling: from enzyme chemistry to proteomic chemistry. Annu. Rev. Biochem. *77*, 383–414.

Dawson, J.E., Seckute, J., De, S., Schueler, S.A., Oswald, A.B., and Nicholson, L.K. (2009). Elucidation of a pH-folding switch in the Pseudomonas syringae effector protein AvrPto. Proc. Natl. Acad. Sci. USA *106*, 8543–8548.

DeYoung, B.J., Qi, D., Kim, S.H., Burke, T.P., and Innes, R.W. (2012). Activation of a plant nucleotide binding-leucine rich repeat disease resistance protein by a modified self protein. Cell. Microbiol. *14*, 1071–1084.

Dowen, R.H., Engel, J.L., Shao, F., Ecker, J.R., and Dixon, J.E. (2009). A family of bacterial cysteine protease type III effectors utilizes acylation-dependent and -independent strategies to localize to plasma membranes. J. Biol. Chem. *284*, 15867–15879.

Edgington, L.E., Verdoes, M., and Bogyo, M. (2011). Functional imaging of proteases: recent advances in the design and application of substrate-based and activity-based probes. Curr. Opin. Chem. Biol. *15*, 798–805.

Hotson, A., and Mudgett, M.B. (2004). Cysteine proteases in phytopathogenic bacteria: identification of plant targets and activation of innate immunity. Curr. Opin. Plant Biol. *7*, 384–390.

Huynh, T.V., Dahlbeck, D., and Staskawicz, B.J. (1989). Bacterial blight of soybean: regulation of a pathogen gene determining host cultivar specificity. Science *245*, 1374–1377.

Iriarte, M., and Cornelis, G.R. (1998). YopT, a new Yersinia Yop effector protein, affects the cytoskeleton of host cells. Mol. Microbiol. *29*, 915–929.

Jenner, C., Hitchin, E., Mansfield, J., Walters, K., Betteridge, P., Teverson, D., and Taylor, J. (1991). Gene-for-gene interactions between *Pseudomonas syringae* pv. *phaseolicola* and Phaseolus. Mol. Plant Microbe Interact. *4*, 553–562.

Johnson, S., Deane, J.E., and Lea, S.M. (2005). The type III needle and the damage done. Curr. Opin. Struct. Biol. *15*, 700–707.

Katagiri, F., Thilmony, R., and He, S.Y. (2002). The *Arabidopsis thaliana-pseudomonas syringae interaction*. Arabidopsis Book *1*, e0039.

Kato, D., Boatright, K.M., Berger, A.B., Nazif, T., Blum, G., Ryan, C., Chehade, K.A.H., Salvesen, G.S., and Bogyo, M. (2005). Activity-based probes that target diverse cysteine protease families. Nat. Chem. Biol. *1*, 33–38.

Kobe, B., and Kemp, B.E. (1999). Active site-directed protein regulation. Nature *402*, 373–376.

Labes, M., Pühler, A., and Simon, R. (1990). A new family of RSF1010-derived expression and lac-fusion broad-host-range vectors for gram-negative bacteria. Gene *89*, 37–46.

Loquet, A., Sgourakis, N.G., Gupta, R., Giller, K., Riedel, D., Goosmann, C., Griesinger, C., Kolbe, M., Baker, D., Becker, S., and Lange, A. (2012). Atomic model of the type III secretion system needle. Nature *486*, 276–279.

Mackey, D., Belkhadir, Y., Alonso, J.M., Ecker, J.R., and Dangl, J.L. (2003). Arabidopsis RIN4 is a target of the type III virulence effector AvrRpt2 and modulates RPS2-mediated resistance. Cell *112*, 379–389.

Nimchuk, Z., Marois, E., Kjemtrup, S., Leister, R.T., Katagiri, F., and Dangl, J.L. (2000). Eukaryotic fatty acylation drives plasma membrane targeting and enhances function of several type III effector proteins from *Pseudomonas syringae*. Cell *101*, 353–363.

Penaloza-Vazquez, A., Preston, G.M., Collmer, A., and Bender, C.L. (2000). Regulatory interactions between the Hrp type III protein secretion system and coronatine biosynthesis in *Pseudomonas syringe* pv. *tomato* DC3000. Micobiol. *146*, 2447–2456.

Puri, N., Jenner, C., Bennett, M., Stewart, R., Mansfield, J., Lyons, N., and Taylor, J. (1997). Expression of avrPphB, an avirulence gene from *Pseudomonas syringae* pv. *phaseolicola*, and the delivery of signals causing the hypersensitive reaction in bean. Mol. Plant Microbe Interact. *10*, 247–256.

Quirino, B.F., and Bent, A.F. (2003). Deciphering host resistance and pathogen virulence: the Arabidopsis/Pseudomonas interaction as a model. Mol. Plant Pathol. *4*, 517–530.

Rawlings, N.D., Barrett, A.J., and Bateman, A. (2012). MEROPS: the database of proteolytic enzymes, their substrates and inhibitors. Nucleic Acids Res. *40*(Database issue), D343–D350.

Richau, K.H., Kaschani, F., Verdoes, M., Pansuriya, T.C., Niessen, S., Stüber, K., Colby, T., Overkleeft, H.S., Bogyo, M., and Van der Hoorn, R.A. (2012). Subclassification and biochemical analysis of plant papain-like cysteine proteases displays subfamily-specific characteristics. Plant Physiol. *158*, 1583–1599.

Serim, S., Haedke, U., and Verhelst, S.H.L. (2012). Activity-based probes for the study of proteases: recent advances and developments. ChemMedChem *7*, 1146–1159.

Shao, F., Merritt, P.M., Bao, Z., Innes, R.W., and Dixon, J.E. (2002). A Yersinia effector and a Pseudomonas avirulence protein define a family of cysteine proteases functioning in bacterial pathogenesis. Cell *109*, 575–588.

Shao, F., Golstein, C., Ade, J., Stoutemyer, M., Dixon, J.E., and Innes, R.W. (2003). Cleavage of Arabidopsis PBS1 by a bacterial type III effector. Science *301*, 1230–1233.

Simonich, M.T., and Innes, R.W. (1995). A disease resistance gene in Arabidopsis with specificity for the avrPph3 gene of *Pseudomonas syringae* pv. *phaseolicola*. Mol. Plant Microbe Interact. *8*, 637–640.

Singer, A.U., Desveaux, D., Betts, L., Chang, J.H., Nimchuk, Z., Grant, S.R., Dangl, J.L., and Sondek, J. (2004). Crystal structures of the type III effector protein AvrPphF and its chaperone reveal residues required for plant pathogenesis. Structure *12*, 1669–1681.

Tampakaki, A.P., Bastaki, M., Mansfield, J.W., and Panopoulos, N.J. (2002). Molecular determinants required for the avirulence function of AvrPphB in bean and other plants. Mol. Plant Microbe Interact. *15*, 292–300.

Turk, V., Stoka, V., Vasiljeva, O., Renko, M., Sun, T., Turk, B., and Turk, D. (2012). Cysteine cathepsins: from structure, function and regulation to new frontiers. Biochim. Biophys. Acta *1824*, 68–88.

Wenig, K., Chatwell, L., von Pawel-Rammingen, U., Björck, L., Huber, R., and Sondermann, P. (2004). Structure of the streptococcal endopeptidase IdeS, a cysteine proteinase with strict specificity for IgG. Proc. Natl. Acad. Sci. USA *101*, 17371–17376.

Zhang, J., Li, W., Xiang, T., Liu, Z., Laluk, K., Ding, X., Zou, Y., Gao, M., Zhang, X., Chen, S., et al. (2010). Receptor-like cytoplasmic kinases integrate signaling from multiple plant immune receptors and are targeted by a *Pseudomonas syringae* effector. Cell Host Microbe *7*, 290–301.

Zhu, M., Shao, F., Innes, R.W., Dixon, J.E., and Xu, Z. (2004). The crystal structure of Pseudomonas avirulence protein AvrPphB: a papain-like fold with a distinct substrate-binding site. Proc. Natl. Acad. Sci. USA *101*, 302–307.

